

## Enhancement of the in-field $J_c$ of MgB<sub>2</sub> via SiCl<sub>4</sub> doping

Xiao-Lin Wang,<sup>1,\*</sup> S. X. Dou,<sup>1</sup> M. S. A. Hossain,<sup>1</sup> Z. X. Cheng,<sup>1</sup> X. Z. Liao,<sup>2</sup> S. R. Ghorbani,<sup>1,3</sup> Q. W. Yao,<sup>1</sup>  
J. H. Kim,<sup>1</sup> and T. Silver<sup>1</sup>

<sup>1</sup>*Institute for Superconducting and Electronic Materials, University of Wollongong, Wollongong, New South Wales 2522, Australia*

<sup>2</sup>*School of Aerospace, Mechanical & Mechatronic Engineering, Building J07, The University of Sydney, New South Wales 2006, Australia*

<sup>3</sup>*Department of Physics, Sabzevar Tarbiat Moallem University, P.O. Box 397, Sabzevar, Iran*

(Received 22 December 2009; revised manuscript received 7 March 2010; published 15 June 2010)

We present the following results. (1) We introduce a doping source for MgB<sub>2</sub>, liquid SiCl<sub>4</sub>, which is free of C, to significantly enhance the irreversibility field ( $H_{irr}$ ), the upper critical field ( $H_{c2}$ ), and the critical current density ( $J_c$ ) with a little reduction in the critical temperature ( $T_c$ ). (2) Although Si can not be incorporated into the crystal lattice, a significant reduction in the  $a$ -axis lattice parameter was found, to the same extent as for carbon doping. (3) Based on the first-principles calculation, it is found that it is reliable to estimate the C concentration just from the reduction in the  $a$ -lattice parameter for C-doped MgB<sub>2</sub> polycrystalline samples that are prepared at high sintering temperatures, but not for those prepared at low sintering temperatures. Strain effects and magnesium deficiency might be reasons for the  $a$ -lattice reduction in non-C or some of the C-added MgB<sub>2</sub> samples. (4) The SiCl<sub>4</sub>-doped MgB<sub>2</sub> shows much higher  $J_c$  with superior field dependence above 20 K compared to undoped MgB<sub>2</sub> and MgB<sub>2</sub> doped with various carbon sources. (5) We introduce a parameter, RHH ( $H_{c2}/H_{irr}$ ), which can clearly reflect the degree of flux-pinning enhancement, providing us with guidance for further enhancing  $J_c$ . (6) It was found that spatial variation in the charge-carrier mean free path is responsible for the flux-pinning mechanism in the SiCl<sub>4</sub> treated MgB<sub>2</sub> with large in-field  $J_c$ .

DOI: [10.1103/PhysRevB.81.224514](https://doi.org/10.1103/PhysRevB.81.224514)

PACS number(s): 74.70.Ad, 74.25.Sv

### I. INTRODUCTION

Magnesium diboride superconductor (MgB<sub>2</sub>),<sup>1</sup> with a much higher superconducting transition temperature ( $T_c$ ) of 40 K and lower cost than conventional low-temperature superconductors ( $T_c < 25$  K), has great potential for large-scale and microelectronic applications at temperatures far above that of liquid helium (4.2 K). For practical applications that require carrying large supercurrents in the presence of magnetic field, improvement in the critical current density ( $J_c$ ) has been the key research topic for MgB<sub>2</sub>, although the weak link problem is almost negligible<sup>2</sup> compared to the high- $T_c$  cuprate superconductors. The irreversibility field,  $H_{irr}$ , is the maximum field at which MgB<sub>2</sub> loses its supercurrent. There are three ways to increase  $H_{irr}$ : (1) increasing  $T_c$ ; (2) increasing the upper critical field,  $H_{c2}$ ; and (3) introducing effective pinning centers to enhance the flux pinning if  $H_{c2}$  is fixed. However, the  $T_c$  of MgB<sub>2</sub> always decreases for the various dopants that can substitute into either Mg or B sites and can be significantly reduced to very low temperatures far below 40 K,<sup>3</sup> limiting applications at higher temperatures above 20 K. The enhancement of  $H_{c2}$  has been very successful via various types of chemical doping, such as nano-SiC, Si, and C (Refs. 4–11) carbohydrates<sup>12</sup> containing C, H, and O and liquid additive, silicone oil containing Si, C, H, and O.<sup>13</sup>

So far, it has been widely accepted that, among all the chemical dopants, carbon is the most successful doping element for significantly enhancing  $H_{c2}$ , depending on the carbon doping level. The reason is that the B sites are partially occupied by carbon and cause stronger intraband electron scattering in the  $\sigma$  band than the  $\pi$  intraband electron scattering at high temperature, which leads to a positive curvature of  $H_{c2}$  at temperatures close to  $T_c$ , and therefore en-

hances  $H_{c2}$  significantly. In addition, it was pointed out that achieving high  $H_{c2}$  requires the modification of intraband and interband scattering in both  $\sigma$  and  $\pi$  bands.<sup>14</sup> However, the disadvantage of carbon doping is that it leads to a significant drop in  $T_c$  from 39 K down to near 10 K, for carbon content up to 20%.<sup>15</sup> This means that a small amount of C can significantly increase the  $H_{c2}$ , but with large sacrifices in  $T_c$ . As a consequence, the significant reduction in  $T_c$  due to C doping hinders MgB<sub>2</sub> from applications above 20 K, which should be the lowest temperature limit at which the MgB<sub>2</sub> is most likely to be useful in liquid-helium free magnetic resonance imaging devices. As for the third approach, if both the  $T_c$  and the  $H_{c2}$  are fixed, the  $H_{irr}$  can be moved up by introducing effective pinning centers. This is the case where there is enhancement of effective flux pinning.

Furthermore, it should be pointed out that there are three issues to do with pinning enhancement that have to be clarified for MgB<sub>2</sub> doping with C using various carbon sources. (1) What role do C and the residual C play in flux pinning? (2) Does C really occupy B sites in the case of samples made at low sintering temperatures? (3) Can we use empirical rules based on C-doped MgB<sub>2</sub> single crystals or the reduction in the  $a$  lattice parameter to estimate the carbon concentration in the samples doped using various carbon sources? (4) Can we find another dopant that is capable of enhancing  $J_c$  as much as C does, but without degradation in  $T_c$ ? (5) What has really been improved for all the MgB<sub>2</sub> in all the chemical doping studies? Or, what are the effective approaches to judge whether or not effective flux pinning has been introduced into MgB<sub>2</sub>? The above questions are the motivations behind this work on introducing a Si source, liquid SiCl<sub>4</sub>, which is free of C, and all these issues are discussed.

The differences between the SiCl<sub>4</sub> and all the other above-mentioned doping chemicals are as follows. (1) SiCl<sub>4</sub> does not produce C at all, while all the other  $J_c$  enhancing dopants

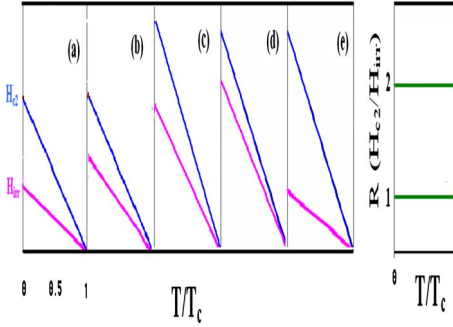


FIG. 1. (Color online) Schematic showing magnetic fields of  $H_{c2}$  and  $H_{irr}$  lines as a function of reduced temperature  $T/T_c$  for different types of samples (a)–(e). RHH ratio as a function of reduced temperature (f), showing cases where the  $H_{irr}$  and the  $H_{c2}$  lines coincide (RHH=1) and where there is fairly weak pinning (RHH=2). For samples with good pinning performance, the RHH values should be located close to 1.

contain carbon. (2) In addition to silicone oil,<sup>13</sup>  $\text{SiCl}_4$  is a typical inorganic liquid containing Si. It is widely used to produce Si nanowires as one of the starting precursors. Therefore, it is an ideal inorganic liquid for doping  $\text{MgB}_2$ . (3) As it is a liquid under ambient conditions, it offers a great advantage in terms of very homogeneous mixing with solid-state particles such as boron, as compared to the problem of mixing two solid-state materials. (4)  $\text{SiCl}_4$  can decompose quickly and form very fine  $\text{SiO}_2$  when exposed to the air.

The RRR ratio, i.e., the ratio of the resistivity at 300 K to that at  $T_c$  has been widely used as a parameter to reflect the degree of electron scattering. It is well known that the RRR ratio is decreased in the dirty-band case. It was pointed out that in the dirty case, the electric current is carried only by the  $\sigma$  bands, since the impurity scattering in the  $\pi$  band is very high.<sup>16</sup> It is believed that the RRR ratio is also related to flux pinning. However, in most cases, the RRR ratios only give an indication of the electron scattering and may have no correlation with the degree of pinning. Here, we introduce another ratio, RHH, the ratio of  $H_{c2}(T)$  to  $H_{irr}(T)$ . As shown in Figs. 1(a) and 1(b), for a sample with a fixed  $H_{c2}$ , the position of the irreversibility line reflects the degree of flux pinning. A smaller distance between the  $H_{irr}$  and the  $H_{c2}$  lines reflects stronger flux pinning while a large distance means weaker pinning. Generally,  $H_{irr}$  rises in proportion to any increase in  $H_{c2}$ , because the same defects that are effective for electron scattering also tend to pin flux. In the case of  $\text{MgB}_2$  with a higher  $H_{c2}$ , however [see Figs. 1(c) and 1(d)], the  $H_{irr}$  line may not necessarily increase in proportion to the increase in  $H_{c2}$ . In this case, flux pinning is not enhanced, even though the absolute value of  $H_{irr}$  may be higher than that of  $\text{MgB}_2$  with lower  $H_{c2}$ . It is obvious that if the RHH value is close to 1, the flux pinning, and thus  $H_{irr}$ , reaches its limit. In other words, if effective pinning centers are present in a  $\text{MgB}_2$  sample, the RHH should be as close to 1 as possible. If RHH is greater than 2, that means an  $H_{irr}$  that is only half as great as  $H_{c2}$ . If the  $\text{RHH} \gg 2$ , one can say that the flux pinning is very weak.

In this work, we found that liquid  $\text{SiCl}_4$  enhanced significantly the irreversibility field ( $H_{irr}$ ), the upper critical field

( $H_{c2}$ ), and the critical current density ( $J_c$ ) with little reduction in the critical temperature ( $T_c$ ). Although Si cannot be incorporated into the crystal lattice, a reduction in the  $a$ -axis lattice parameter was found. At  $T > 20$  K, the  $\text{SiCl}_4$ -doped  $\text{MgB}_2$  shows much higher  $J_c$  than undoped  $\text{MgB}_2$  and  $\text{MgB}_2$  doped with various carbon sources. A parameter, RHH ( $H_{c2}/H_{irr}$ ), is introduced to reflect on the degree of flux-pinning enhancement. It was found that spatial variation in the charge-carrier mean free path is responsible for the flux-pinning mechanism in the  $\text{SiCl}_4$ -doped  $\text{MgB}_2$ .

## II. EXPERIMENTALS

The amorphous boron powders were mixed with a few drops of  $\text{SiCl}_4$  (with the appropriate amount calculated to correspond to about 10 wt % Si) so that a very thin layer of  $\text{SiO}_2$  coated onto the surface of the B particles. This took place instantly at room temperature, as the  $\text{SiCl}_4$  decomposed to HCl and formed  $\text{SiO}_2$ . The HCl is highly volatile and can evaporate instantly. This reaction and coating process were carefully carried out in a fume cupboard. The Mg powder was then mixed well with the B powder coated with  $\text{SiO}_2$ . The mixed powders were pelletized and sintered *in situ* at temperatures in the range of 650–750 °C for just 10 min in pure Ar gas. Extra Mg was also added to compensate for the lost of Mg during the sintering. The  $\text{MgB}_2$  samples made using  $\text{SiCl}_4$  as silicon source are referred to as  $\text{SiCl}_4$ - $\text{MgB}_2$  in this study. The x-ray diffraction (XRD) and the transmission electron microscopy (TEM) results revealed that all the samples were crystallized in the  $\text{MgB}_2$  structure as the major phase. A few impurity lines from MgO and  $\text{Mg}_2\text{Si}$  were observed.

The resistivity measurements were carried out by using a physical properties measurement system (PPMS, Quantum Design) in the field ranging from 0 up to 8.7 T. The magnetic hysteresis loops were measured using a magnetic properties measurement system (MPMS, Quantum Design). The critical current density was calculated by using the Bean approximation.

The first-principles calculations were performed using a density-functional theory.<sup>6</sup> A cut-off energy of 340 eV and a self-consistent field tolerance of  $10^{-6}$  eV/atom were used. The ultrasoft pseudopotentials basis set and the general gradient approximation corrected Perdew, Burke, and Enzerhof functional<sup>17</sup> were adopted. The calculations were performed on a  $2 \times 2 \times 2$  supercell containing 8 Mg and 16 B atoms. C or O individual doping effect on the lattice parameters was calculated by replacing B using one C or one O atom, respectively. This corresponds to 6% C or 6% O doping on B site. A magnesium vacancy was created by removing one Mg in the supercell, leading to 12% Mg vacancy. The lattice parameters were obtained through geometrical optimization.

## III. RESULTS AND DISCUSSION

The calculated XRD patterns using Rietveld refinement fit very well with the observed ones. The refined and observed XRD patterns for the 10 wt %  $\text{SiCl}_4$  added sample are shown in Fig. 2. The lattice parameters obtained from the

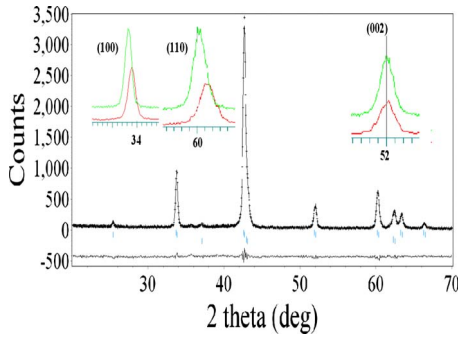


FIG. 2. (Color online) XRD pattern of the observed (crosses), calculated (solid line), and difference (bottom solid line) diffraction profiles at 300 K for  $MgB_2$  with 10 wt %  $SiCl_4$  added. The upper and the lower peak markers relate to  $MgB_2$  and  $MgO$ , respectively. The insets show key XRD peaks for the doped (green, larger peaks) and the pure (red, smaller peaks) samples.

refinement revealed that the  $a$ -lattice parameter had been reduced from 3.085 to 3.077 Å for the 10 wt %  $SiCl_4$ -doped samples as compared to the pure ones. The reduction in the  $a$ -lattice parameter is clearly indicated by the shift of both the (100) and the (110) peaks to low-diffraction angles while the (002) peak position remains almost unchanged, as illustrated in the insets in Fig. 2.

It should be noted that the  $a$ -lattice parameter is almost the same as what is commonly seen in so-called C-doped  $MgB_2$  using various C sources. It was found that the  $a$ -lattice parameter decreased as C content  $x$  in  $Mg(B_{1-x}C_x)$  increased.<sup>10,15</sup> Figure 3 displays the reduction in the  $a$ -lattice parameter from some typical  $MgB_2$  doped with various C sources<sup>4,18–21</sup> and heat treated at low sintering temperatures and compares them with the  $SiCl_4$ - $MgB_2$  sample. We can see that all the C-doped samples have almost the same  $a$  value and that, surprisingly, the  $SiCl_4$ - $MgB_2$  sample shows the largest reduction in the  $a$ -lattice parameter. It is obvious that it would be definitely unreliable to calculate the carbon concentration in C-doped  $MgB_2$  just from the reduction in the  $a$ -lattice parameter. In other words, reduction in the  $a$ -lattice parameter cannot be used as a criterion to judge if the C really is substituted onto boron sites. This lack of correspondence is particularly likely to hold true for samples made at low sintering temperatures with low C doping content and slightly decreased  $T_c$ . However, for high sintering tempera-

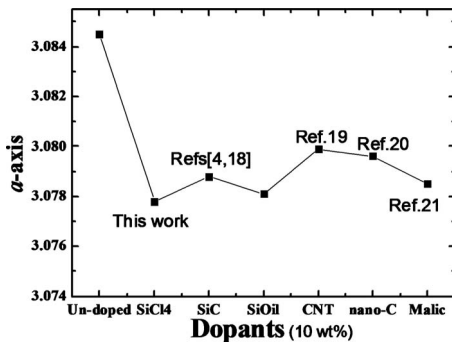


FIG. 3.  $a$ -axis lattice parameter in various doped and undoped  $MgB_2$  samples.

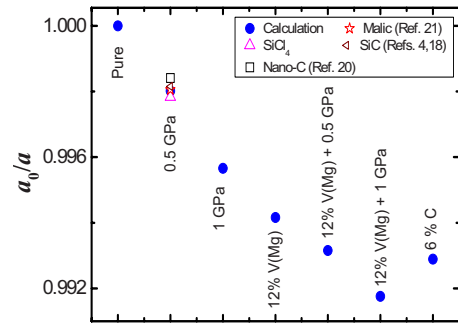


FIG. 4. (Color online) The ratio of  $a/a_0$  ( $a_0$  is the  $a$ -lattice parameter of the stoichiometric  $MgB_2$  unit cell) calculated from first-principles calculations for various conditions. 12% V(Mg) means that the magnesium vacancy is 12%.

ture (close to 1000 °C), if both  $T_c$  and the  $a$ -lattice parameter are reduced significantly, estimation of the C content from the  $a$ -lattice parameter should be reasonable.

Two facts were obtained from the Rietveld refinement. (1) The Mg is very deficient. The occupancies of Mg are about 0.91 and 0.92 for the pure and the  $SiCl_4$ - $MgB_2$  samples. (2) The  $c$ -lattice parameter for  $SiCl_4$ - $MgB_2$  is 3.526 Å, slightly greater than for the pure sample (3.524 Å). In order to understand what could cause the changes in the  $a$ -lattice parameter, we carried out a first-principles calculation for the following possibilities: (1) Mg deficiency; (2) oxygen occupancy on B sites; (3) strain/pressure effect; and (4) C doping on B sites.

For case (2), the oxygen occupancy at B sites, our calculation indicates that both the  $a$  and  $c$  lattice parameters fluctuate when oxygen occupies B sites for different oxygen doping levels. Therefore, it is not clear whether or not the reduction in the  $a$ -lattice reduction observed in our  $SiCl_4$ - $MgB_2$  is caused by any possible oxygen occupancy on B site. The ratio of  $a/a_0$  ( $a_0$  is the  $a$ -lattice parameter of stoichiometric  $MgB_2$  unit cell) calculated from the first-principles calculations for the cases (1), (3), and (4) is shown in Fig. 4. It can be seen that the reduction in the  $a$ -lattice parameter can be caused not only by the carbon substitution but also by magnesium deficiency and strain/pressure effect. The experimental data on the  $a/a_0$  from  $MgB_2$  samples doped with different carbon source and our  $SiCl_4$  treated samples are also shown in the Fig. 4. It is found that all these samples show the same  $a/a_0$  values as that of  $MgB_2$  sample under strain/pressure of 0.5 GPa.

The almost the same level of Mg deficiency is present for both undoped and  $SiCl_4$  treated  $MgB_2$ . So, the Mg vacancies cannot be the origin of the  $a$ -lattice reduction. One may argue that this is not necessarily a proof that this reduction is mainly caused by the strain/pressure effect. However, based on what we have calculated for various possible cases, the internal strain or internal pressure plus the Mg vacancies might be one of the reasons for the  $a$ -lattice reduction for both undoped and  $SiCl_4$ - $MgB_2$  samples. Further investigations on what really causes the  $a$ -lattice reduction in Si added and other noncarbon-doped  $MgB_2$  samples are necessary.

It should also be noted that the  $a$ -lattice parameter can be further reduced for non-C containing  $MgB_2$  with more Mg

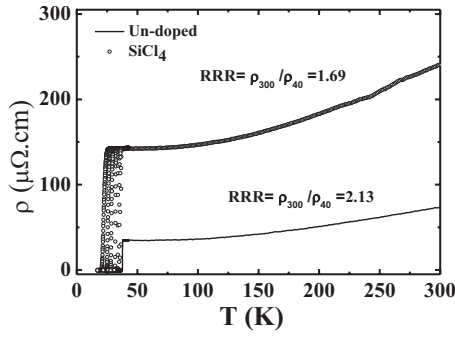


FIG. 5. Temperature dependence of the resistivity measured at fields up to 8.7 T for 10 wt % SiCl<sub>4</sub> doped and pure MgB<sub>2</sub>.

deficiency and a larger strain effect. It implies that it may not be reliable to estimate the C concentration just from the reduction in the *a*-lattice parameter in some of the C-doped MgB<sub>2</sub> polycrystalline samples, in particular, those prepared at low sintering temperatures. This may be true for samples where the strain is caused by the element added to the sample but not due to the synthesis parameters because in this case the *a*-lattice reduction should also be present in the pure MgB<sub>2</sub> sample used as reference. However, this may not be true for other cases, in particular, for those polycrystalline samples prepared at higher temperatures.<sup>6,11</sup>

Figure 5 shows the resistance versus temperature curves (*R-T*) over the temperature range from 30 to 300 K. The resistivity at 40 K increased from 24 μΩ cm for the pure MgB<sub>2</sub> to 64 μΩ cm for the doped MgB<sub>2</sub>. The *T<sub>c</sub>* values and residual resistivity ratios,  $R(300\text{ K})/R(T_c)$  (RRR), were obtained to be 38.2 and 36.2 K, 2.13 and 1.69, for the pure and SiCl<sub>4</sub>-MgB<sub>2</sub> samples, respectively. Therefore, the large variation in the residual resistivities and the reduced RRR values indicate that the intraband scattering rate, which does not strongly affect on *T<sub>c</sub>* depression, is enhanced in the sample with the addition of SiCl<sub>4</sub>.

The magnetic field dependence of *J<sub>c</sub>* at 20 and 5 K is shown in Fig. 6. For comparison purposes, the data from an MgB<sub>2</sub> sample doped with malic acid (C<sub>4</sub>H<sub>6</sub>O<sub>5</sub>), a typical carbon source, is also included in the figure. It is interesting to note that the *J<sub>c</sub>* at 20 K for the SiCl<sub>4</sub>-MgB<sub>2</sub> sample at both low and high fields is higher than for both the pure and the malic acid-doped MgB<sub>2</sub> samples, which were made under the same conditions as the SiCl<sub>4</sub>-MgB<sub>2</sub>. It should be noted that the *J<sub>c</sub>* of the SiCl<sub>4</sub>-MgB<sub>2</sub> is one order of magnitude higher than for the pure MgB<sub>2</sub> at 5 T and the malic acid-doped MgB<sub>2</sub> at 6 T. The *J<sub>c</sub>* values of the 10 wt % SiCl<sub>4</sub> added MgB<sub>2</sub> are over  $1-2 \times 10^4$  A/cm<sup>2</sup> at 8 T and 5 K, more than one order of magnitude higher than for the pure MgB<sub>2</sub>, and almost the same at low fields and comparable to the malic acid-doped MgB<sub>2</sub> at high fields. These results indicate that the SiCl<sub>4</sub> has the advantage of large *J<sub>c</sub>* at high temperatures over C-doped MgB<sub>2</sub>, as it only decreases the *T<sub>c</sub>* slightly to 36.7 K, compared to 33 K for the malic acid-doped MgB<sub>2</sub>.

The *H<sub>c2</sub>* and *H<sub>irr</sub>* were determined from the 90% or 10% drop in the normal-state resistivity values in the *R-T* curves. Figure 7 shows the *H<sub>c2</sub>* and *H<sub>irr</sub>* versus normalized temperature *T/T<sub>c</sub>*. The *H<sub>c2</sub>* and *H<sub>irr</sub>* values of the undoped sample are

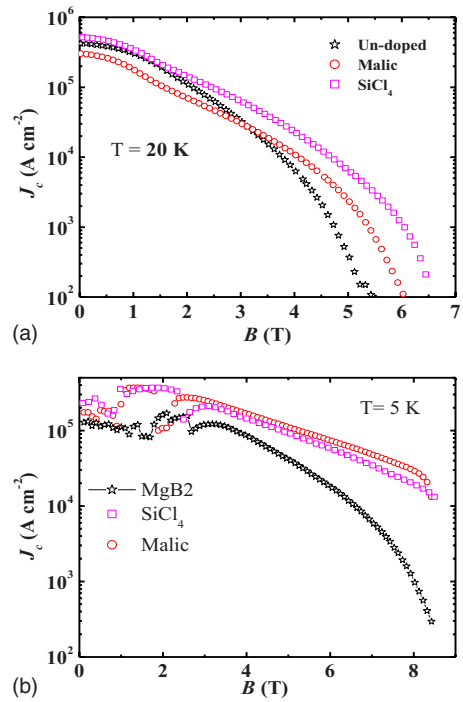


FIG. 6. (Color online) Magnetic field dependence of the critical current at (a) 20 K and (b) 5 K for pure, 10 wt % SiCl<sub>4</sub> doped, and malic acid-doped MgB<sub>2</sub>.

also included in Fig. 7 for comparison. Significantly enhanced *H<sub>irr</sub>* and *H<sub>c2</sub>* are clearly observed for the SiCl<sub>4</sub>-doped MgB<sub>2</sub> sample. The above results reveal that the doped MgB<sub>2</sub> has higher *H<sub>irr</sub>* values compared to the undoped samples that were processed under the same fabrication conditions.

Now let us consider if the SiCl<sub>4</sub> results in the enhancement of flux pinning. We need to know if the enhanced in-field *J<sub>c</sub>* or *H<sub>irr</sub>* is caused by the enhancement of *H<sub>c2</sub>* or the introduction of more effective pinning centers compared to the undoped MgB<sub>2</sub> samples. As we have explained in the introduction section, we calculated the ratio,  $RHH = H_{c2}/H_{irr}$  for the SiCl<sub>4</sub>-MgB<sub>2</sub> sample. The results are shown in Fig. 8. As was discussed earlier, if the RHH value is close to 1, it means that flux pinning is very strong. As can be seen from Fig. 8, the RHH values for the SiCl<sub>4</sub> sample are the same as for the undoped MgB<sub>2</sub>. This means that the *H<sub>irr</sub>* enhancement is not due to the introduction of extra effective

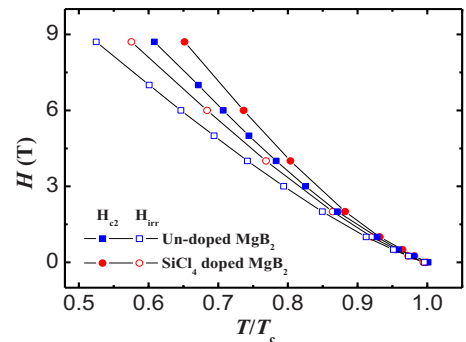


FIG. 7. (Color online) Temperature dependence of *H<sub>irr</sub>* and *H<sub>c2</sub>* for pure MgB<sub>2</sub> and SiCl<sub>4</sub>-MgB<sub>2</sub>.

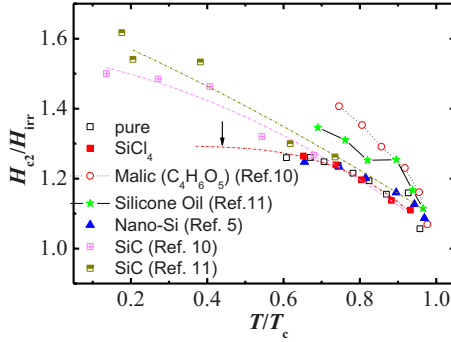


FIG. 8. (Color online) RHH ratio as a function of reduced temperature for various  $\text{MgB}_2$  samples doped with 10 wt % chemicals and sintered at the same temperature.

pinning centers, instead, its enhancement is a result of the  $H_{c2}$  enhancement. We have used this RHH ratio to evaluate what happened in the C-doped samples with malic acid ( $\text{C}_4\text{H}_6\text{O}_5$ ),<sup>12</sup> silicone oil, and nano-SiC doping.<sup>10,11,13</sup> We can see that their RHH lines are above those of both pure and  $\text{SiCl}_4$ -doped samples. This clearly demonstrates that the enhancement of  $J_c$  in malic acid-, silicone-oil-, or nano-SiC-doped  $\text{MgB}_2$  is caused by an increase in  $H_{c2}$  rather than flux-pinning enhancement. It should be noted that the values of  $H_{c2}/H_{c2}^{irr}$  increase with decreasing temperature for all the doped samples given in Fig. 8, indicating that the effective pinning becomes weaker at low temperatures. It is interesting to note that the nano-Si-doped  $\text{MgB}_2$  has the same RHH values as  $\text{SiCl}_4$  ( $T/T_c > 0.6$ ) indicating that nano-Si doping<sup>5</sup> enhances  $H_{c2}$  without reducing flux-pinning effect compared to the  $\text{MgB}_2$  doping with different C sources. The RHH values or RHH lines give us some guidance on how to further enhance the  $J_c$  for  $\text{MgB}_2$ . For C doping, it is clear that we still have plenty of room to enhance the in-field  $J_c$ , if we can reduce the RHH values further or keep it constant for low temperatures by optimizing the fabrication conditions (as shown by the curve indicated by the arrow in Fig. 8).

We now discuss what causes the enhancement of  $H_{c2}$  in the  $\text{SiCl}_4$ - $\text{MgB}_2$ . We first look at the grain sizes, based on the full width at half maximum of the XRD peaks. The diffraction peaks are observed to be broadened, compared with undoped samples, indicating that the grain sizes are reduced and considerable strain has been introduced.

Figure 9(a) shows a TEM image for the  $\text{SiCl}_4$ - $\text{MgB}_2$  sample. The sample has an average grain size of several tens of nanometer and contains a high density of defects, such as dislocations and heavy strains in the lattice. Under high magnification (b) we can see a large density of  $\text{MgO}$  clusters or  $\text{Mg}(\text{B},\text{O})_2$  precipitates<sup>22</sup> with sizes of 1–3 nm that have been embedded in individual grains. These clusters were obviously introduced from oxygen released from  $\text{SiO}_2$  in the initial sample sintering process. The small drop in the  $T_c$  for the  $\text{SiCl}_4$ -doped sample is caused by both Mg and B deficiency as a result of the formation of  $\text{Mg}_2\text{Si}$  and  $\text{Mg}(\text{B},\text{O})_2$  precipitates, respectively, and the enhanced electron scattering from the both  $\text{Mg}_2\text{Si}$  and  $\text{Mg}(\text{B},\text{O})_2$  impurities.

Based on the facts that the grain sizes are reduced, impurities are in the form of inclusions and crystal imperfections/defects have inhomogeneous distributions, we expect the en-

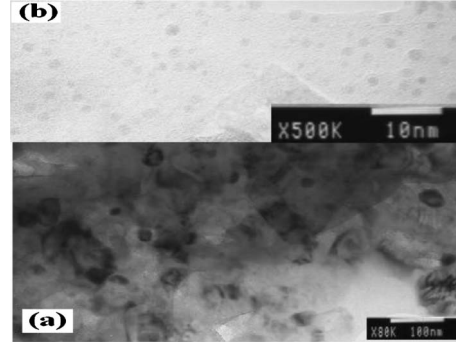


FIG. 9. TEM image of 10 wt %  $\text{SiCl}_4$ -doped  $\text{MgB}_2$ .

hanced scattering and  $H_{c2}$  which have been demonstrated in the previous sections. We now analyze the pinning mechanism in the  $\text{SiCl}_4$ -doped samples.

Two mechanisms of core pinning are predominant in type-II superconductors, i.e.,  $\delta T_c$  and  $\delta l$  pinning.<sup>23</sup> Whereas  $\delta T_c$  pinning is caused by the spatial variation in the GL coefficient associated with disorder in the transition temperature  $T_c$ , variations in the charge-carrier mean free path  $l$  near lattice defects are the main cause of  $\delta l$  pinning. The  $\delta T_c$  and  $\delta l$  pinning mechanisms result in different temperature dependences of  $J_{sv}$ , where  $J_{sv}$  is  $J_c$  in the single-vortex-pinning regime. For  $\delta T_c$  pinning,  $J_{sv} \propto (1-t^2)^{7/6}(1+t^2)^{5/6}$  with  $t = T/T_c$  while for the case of  $\delta l$  pinning,  $J_{sv} \propto (1-t^2)^{2/5}(1+t^2)^{-1/2}$ . Taking into account collective pinning theory,<sup>24</sup>  $J_c$  is field independent when the applied field is lower than a crossover field  $B_{sb}$  at which the dominant pinning mechanism changes from single vortex to small bundle pinning. When the single-vortex-pinning mechanism is dominant  $B_{sb} \propto$  the product of  $J_{sv}$  and  $B_{c2}$ . The following  $B_{sb}$  temperature dependence can be obtained:<sup>25</sup>

$$B_{sb}(T) = B_{sb}(0) \left( \frac{1-t^2}{1+t^2} \right)^\nu,$$

where  $\nu=2/3$  and 2 for  $\delta T_c$  and  $\delta l$  pinning, respectively.

The curves of  $B_{sb}(T)$  for  $\delta T_c$  and  $\delta l$  pinning are shown in Fig. 10. The curvature is positive for  $\delta T_c$  pinning while the curvature associated with  $\delta l$  pinning is negative. It is clear that the  $B_{sb}(T)$ , showing a negative curvature with  $\nu=2$  is in

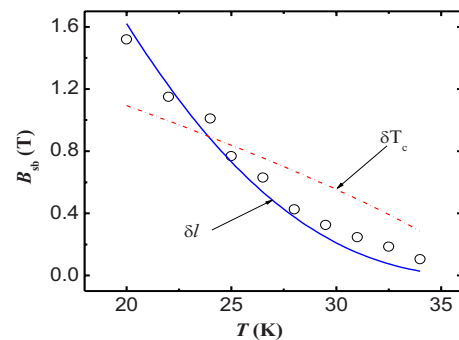


FIG. 10. (Color online) Temperature dependence of the crossover field  $B_{sb}$  for the 10 wt %  $\text{SiCl}_4$ -doped sample with the  $\delta l$  pinning curve with  $\nu=2$  and the  $\delta T_c$  pinning curve with  $\nu=3/2$ .

good agreement with the experimental data. This strongly suggests that  $\delta l$  pinning is the dominant pinning mechanism in our  $\text{SiCl}_4\text{-MgB}_2$  sample. It is believed that the nano-MgO inclusions with variable distances and sizes (1–10 nm) shown in Fig. 9(b) are the main type of defect and the reason for the variation in the charge-carrier mean free path  $l$ .

In summary, we have studied the superconductivity properties and flux-pinning mechanism of the liquid  $\text{SiCl}_4$ -doped  $\text{MgB}_2$ . We found that this dopant enhanced significantly the irreversibility field ( $H_{\text{irr}}$ ), the upper critical field ( $H_{c2}$ ), and the critical current density ( $J_c$ ) with little reduction in the critical temperature ( $T_c$ ). Although Si cannot be incorporated into the crystal lattice, a reduction in the  $a$ -axis lattice parameter was found. Strain effects and magnesium deficiency

might be reasons for the  $a$ -lattice reduction in the samples or other non-C or some of C-doped  $\text{MgB}_2$  polycrystalline samples prepared at low sintering temperatures. We introduce a parameter, RHH ( $H_{c2}/H_{\text{irr}}$ ), which can reflect the degree of flux-pinning enhancement and provide us with guidance for further enhancing  $J_c$ . It was found that spatial variation in the charge-carrier mean free path is responsible for the flux-pinning mechanism in the  $\text{SiCl}_4$ -doped  $\text{MgB}_2$ .

#### ACKNOWLEDGMENT

This work is supported by the Australian Research Council.

\*Author to whom correspondence should be addressed; xiaolin@uow.edu.au

- <sup>1</sup>G. J. Nagamatsu, N. Nakagawa, T. Muranaka, Y. Zenitali, and J. Akimitsu, *Nature (London)* **410**, 63 (2001).
- <sup>2</sup>C. Larbalestier, M. O. Rikel, L. D. Cooley, A. A. Polyanskii, J. Y. Jiang, S. Patnaik, X. Y. Cai, D. M. Feldmann, A. Gurevich, A. A. Squitieri, M. T. Naus, C. B. Eom, E. E. Hellstrom, R. J. Cava, K. A. Regan, N. Rogado, M. A. Hayward, T. He, J. S. Slusky, P. Khalifah, K. Inumaru, and M. Haas, *Nature (London)* **410**, 186 (2001).
- <sup>3</sup>R. J. Cava, H. W. Zandbergen, and K. Inumaru, *Physica C* **385**, 8 (2003).
- <sup>4</sup>S. X. Dou, S. Soltanian, J. Horvat, X. L. Wang, S. H. Zhou, M. Ionescu, H. K. Liu, P. Munroe, and M. Tomsic, *Appl. Phys. Lett.* **81**, 3419 (2002).
- <sup>5</sup>X. L. Wang, S. Soltanian, M. James, M. J. Qin, J. Horvat, Q. W. Yao, H. K. Liu, and S. X. Dou, *Physica C* **408-410**, 63 (2004).
- <sup>6</sup>R. H. T. Wilke, S. L. Bud'ko, P. C. Canfield, D. K. Finnemore, R. J. Slupinskas, and S. T. Hannahs, *Phys. Rev. Lett.* **92**, 217003 (2004).
- <sup>7</sup>B. J. Senkowitz, J. E. Giencke, S. Patnaik, C. B. Eom, E. E. Hellstrom, and D. C. Larbalestier, *Appl. Phys. Lett.* **86**, 202502 (2005).
- <sup>8</sup>V. Braccini, A. Gurevich, J. E. Giencke, M. C. Jewell, C. B. Eom, D. C. Larbalestier, A. Pogrebnjakov, Y. Cui, B. T. Liu, Y. F. Hu, J. M. Redwing, Q. Li, X. X. Xi, R. K. Singh, R. Gandikota, J. Kim, B. Wilkens, N. Newman, J. Rowell, B. Moeckly, V. Ferrando, C. Tarantini, D. Marré, M. Putti, C. Ferdeghini, R. Vaglio, and E. Haanappel, *Phys. Rev. B* **71**, 012504 (2005).
- <sup>9</sup>S. K. Chen, M. Wei, and J. L. MacManus-Driscoll, *Appl. Phys. Lett.* **88**, 192512 (2006).
- <sup>10</sup>S. X. Dou, O. Shcherbakova, W. K. Yeoh, J. H. Kim, S. Soltanian, X. L. Wang, C. Senatore, R. Flukiger, M. Dhalle, O. Husnjak, and E. Babic, *Phys. Rev. Lett.* **98**, 097002 (2007).
- <sup>11</sup>A. Serquis, G. Serrano, S. Moreno, L. Civale, B. Maiorov, F. Balakirev, and M. Jaime, *Supercond. Sci. Technol.* **20**, L12 (2007).
- <sup>12</sup>J. H. Kim, S. Zou, M. S. A. Hossain, A. V. Pan, and S. X. Dou, *Appl. Phys. Lett.* **89**, 142505 (2006).
- <sup>13</sup>X. L. Wang, Z. X. Cheng, and S. X. Dou, *Appl. Phys. Lett.* **90**, 042501 (2007).
- <sup>14</sup>A. Gurevich, *Phys. Rev. B* **67**, 184515 (2003).
- <sup>15</sup>S. M. Kazakov, R. Puzniak, K. Rogacki, A. V. Mironov, N. D. Zhigadlo, J. Jun, C. Soltmann, B. Batlogg, and J. Karpinski, *Phys. Rev. B* **71**, 024533 (2005).
- <sup>16</sup>I. I. Mazin, O. K. Andersen, O. Jepsen, O. V. Dolgov, J. Kortus, A. A. Golubov, A. B. Kuz'menko, and D. van der Marel, *Phys. Rev. Lett.* **89**, 107002 (2002).
- <sup>17</sup>M. D. Segall, P. J. D. Lindan, M. J. Probert, C. J. Pickard, P. J. Hasnip, S. J. Clark, and M. C. Payne, *J. Phys.: Condens. Matter* **14**, 2717 (2002); J. P. Perdew, K. Burke, and M. Ernzerhof, *Phys. Rev. Lett.* **77**, 3865 (1996).
- <sup>18</sup>H. Yamada, M. Hirakawa, H. Kumakura, and H. Kitaguchi, *Supercond. Sci. Technol.* **19**, 175 (2006).
- <sup>19</sup>S. X. Dou, W. K. Yeoh, J. Horvat, and M. Ionescu, *Appl. Phys. Lett.* **83**, 4996 (2003).
- <sup>20</sup>W. K. Yeoh, J. Horvat, J. H. Kim, X. Xu, and S. X. Dou, *Appl. Phys. Lett.* **90**, 122502 (2007).
- <sup>21</sup>J. H. Kim, S. X. Dou, M. S. A. Hossain, X. Xu, J. L. Wang, D. Q. Shi, T. Nakane, and H. Kumakura, *Supercond. Sci. Technol.* **20**, 715 (2007).
- <sup>22</sup>X. Z. Liao, A. Serquis, Y. T. Zhu, J. Y. Huang, L. Civale, D. E. Peterson, F. M. Mueller, and H. F. Xu, *J. Appl. Phys.* **93**, 6208 (2003).
- <sup>23</sup>R. Griessen, W. Hai-hu, A. J. J. van Dalen, B. Dam, J. Rector, and H. G. Schnack, *Phys. Rev. Lett.* **72**, 1910 (1994).
- <sup>24</sup>G. Blatter, M. V. Feigel'man, V. B. Geshkenbein, A. I. Larkin, and V. M. Vinokur, *Rev. Mod. Phys.* **66**, 1125 (1994).
- <sup>25</sup>M. J. Qin, X. L. Wang, H. K. Liu, and S. X. Dou, *Phys. Rev. B* **65**, 132508 (2002).